The Astrophysical Journal, 650: L17–L20, 2006 October 10
© 2006. The American Astronomical Society. All rights reserved. Printed in U.S.A.

THE HUBBLE TIME INFERRED FROM 10 TIME DELAY LENSES

Prasenjit Saha,[1,2] Jonathan Coles,[1] Andrea V. Macciò,[1] and Liliya L. R. Williams[3]

Received 2006 May 18; accepted 2006 July 11; published 2006 August 29

ABSTRACT

We present a simultaneous analysis of 10 galaxy lenses having time delay measurements. For each lens, we derive a detailed free-form mass map, with uncertainties, and with the additional requirement of a shared value of the Hubble parameter across all the lenses. We test the prior involved in the lens reconstruction against a galaxy-formation simulation. Assuming a concordance cosmology, we obtain $H_0^{-1} = 13.5^{+2.5}_{-1.3}$ Gyr.

Subject headings: cosmological parameters — galaxies: general — gravitational lensing

1. INTRODUCTION

If an object at cosmological distance is lensed into multiple images, the light-travel time for individual images differs. For variable sources, the differences are observable as time delays. The delays are of order

$$\Delta t \sim \frac{GM}{c^3} \sim (\Delta\theta)^2 H_0^{-1}, \tag{1}$$

where M is the lens mass and $\Delta\theta$ is the image separation (in radians). As Refsdal (1964) first pointed out, the effect provides an independent way of measuring H_0^{-1}. Time delay measurements have made much progress over the past decade, and now at least 15 are available (details below).

While equation (1) provides the order of magnitude, to determine the precise factor relating time delays and H_0^{-1}, one has to model the mass distribution. An observed set of image positions, rings, magnification ratios, and time delays is generically reproducible by many different mass models. This results in a large model-dependent uncertainty on the inferred Hubble parameter, even with perfect lensing data. To appreciate how serious this model dependence is, compare the models of B0957+561 by Kundić et al. (1997) and Bernstein & Fischer (1999): the results are $H_0 = 64 \pm 13$ and 77^{+29}_{-24} km s^{-1} Mpc^{-1}, respectively, both at 95% confidence; the more general models in the latter paper yield *larger* error bars. Alternatively, consider the nice summary in Figure 12 of Courbin (2006) of published H_0 estimates and uncertainties from individual lenses. Among the lenses shown, B1608+656 has all three of its independent time delays measured, B1115+080 has two delays measured, whereas the others have one each. One would expect these two best-measured lenses to be the best constrained. Yet B1608+656 has the largest error bars on H_0 and B1115+080 the second largest. This suggests that in the less-constrained lenses the real uncertainties are much larger but have been underestimated because the fewness of constraints did not force sufficient exploration of model dependence.

A general strategy for dealing with the nonuniqueness problem is to search through a large ensemble of models that can all reproduce the observations (Williams & Saha 2000; Oguri et al. 2004; Jakobsson et al. 2005). In this Letter, we follow such a strategy, simultaneously modeling 10 time delay lenses coupled by a shared Hubble parameter. The basic method is the same as in Saha & Williams (2004) and the accompanying PixeLens code, but a number of refinements have been made.

2. MODELING THE LENSES

Table 1 summarizes the lenses we have used. By "type" we mean the image morphology (Saha & Williams 2003): AD = axial double, ID = inclined double, SQ = short-axis quad, LQ = long-axis quad, and IQ = inclined quad. In B0957+561, two distinct source elements can be identified; both are lensed into ID.

We use PixeLens to generate an ensemble of 200 models. Each model in the ensemble consists of 10 pixelated mass maps and a shared value of H_0^{-1}. In addition to reproducing all the observed image positions and time delays, the mass maps are required to satisfy a prior. Errors in the image positions and time delays are assumed negligible, since they are much smaller than the range of models that reproduce the data. The details and justification of the prior are given in § 2 of Saha & Williams (2004), but basically the mass maps have to be nonnegative and centrally concentrated with a radial profile steeper than $|\theta|^{-0.5}$, since the lenses are galaxies. With one exception, the mass maps are required to have 180° rotation symmetry; only B1608+656 is allowed to be asymmetric, because the lens is known to contain two galaxies. A constant external shear is allowed for the lenses where the morphology shows evidence of external shear (all except B1608+656, B1104−181, and B2149−274). The lensing galaxies in B0957+561 and J0911+055 have cluster environments, but we have not treated these lenses differently. A concordance cosmology with $\Omega_m = 0.3$, $\Omega_\Lambda = 0.7$ is assumed.

We have not included magnification ratios as a constraint, for two reasons: first, optical flux ratios may be contaminated by microlensing (Keeton et al. 2006) and differential extinction; second, even tensor magnifications—that is, relative magnifications along different directions inferred from VLBI maps—are very weakly coupled with time delays (Raychaudhury et al. 2003), because magnification measures the local second derivative of the arrival time. Stellar velocity dispersions are available for some of the lenses, but we do not attempt to incorporate them, because current methods for doing so depend on strong assumptions about the mass distribution (Koopmans et al. 2006).

There are five additional candidates we have postponed modeling. B1830−211 has a time delay measurement (Lovell et al. 1998), but the lens position is uncertain (Courbin et al. 2002; Winn et al. 2002). B0909+532 (Ullán et al. 2006) also has an uncertain galaxy position. For B0435−122 (Kochanek et al. 2006) and J1131−123 (Morgan et al. 2006), our preliminary modeling appeared to imply asymmetric lenses, whereas the

[1] Institute for Theoretical Physics, University of Zürich, Winterthurerstrasse 190, 8057 Zürich, Switzerland.

[2] Astronomy Unit, Queen Mary and Westfield College, University of London, London E1 4NS, UK.

[3] Department of Astronomy, University of Minnesota, 116 Church Street, SE, Minneapolis, MN 55455.

TABLE 1
LENSES AND TIME DELAYS

Object	Type	z_L	z_S	Δt (days)
J0911+055	SQ	0.77	2.80	146 ± 8[a]
B1608+656	IQ	0.63	1.39	32 ± 2, 5 ± 2, 40 ± 2[b]
B1115+080	IQ	0.31	1.72	13 ± 2, 11 ± 2[c,d]
B0957+561	2 × ID	0.36	1.41	423 ± 1[e]
B1104−181	AD	0.73	2.32	161 ± 7[f]
B1520+530	ID	0.71	1.86	130 ± 3[g]
B2149−274	AD	0.49	2.03	103 ± 12[h]
B1600+434	ID	0.42	1.59	51 ± 4[i]
J0951+263	ID	0.24[j]	1.24	16 ± 2[j]
B0218+357	ID	0.68	0.96	10 ± 1[k,l]

[a] From Hjorth et al. (2002).
[b] From Fassnacht et al. (2002).
[c] From Schechter et al. (1997).
[d] From Barkana (1997).
[e] From Oscoz et al. (2001).
[f] From Ofek & Maoz (2003).
[g] From Burud et al. (2002b).
[h] From Burud et al. (2002a).
[i] From Burud et al. (2000).
[j] From Jakobsson et al. (2005).
[k] From Biggs et al. (1999).
[l] From Cohen et al. (2000).

image morphologies suggest fairly symmetric lenses. Finally, J1650+425 had its time delay measured (Vuissoz et al. 2006) as this Letter was being peer-reviewed.

We remark that while PixeLens in scientific terms is essentially the same as in Saha & Williams (2004), it has undergone several technical improvements. The key parameter in the code's performance is the total number of pixels (not pixels per lens), say, P. The memory required scales as P^2 and the time scales as P^3. The maximum usable P is in practice dictated not by time or memory but by the accumulation of round-off error. Our earlier paper attempted only three or four lenses at a time, going up to $P \simeq 600$. After improving the control of round-off error, PixeLens can now go up to $P \simeq 2000$ and beyond without difficulty. Meanwhile improving the memory management and implementing multithreading (which parallelizes the computation if run on a shared-memory multiprocessor machine) and newer hardware have more than compensated for the P^3 increase in arithmetic.

We have previously done two different tests of the general method. In Saha et al. (2006), the algorithm is tested by feeding time delays sampled from a model ensemble back into PixeLens and then recovering the model H_0^{-1}. This showed that any biases introduced by the ensemble-generating process have affected H_0^{-1} by less than 5% but did not test the prior. Williams & Saha (2000) presented a blind test where one author simulated data using simple model galaxies and a secret fictional value of H_0, and the other author recovered that value within uncertainties using an ancestor of PixeLens. That provided a basic test of the whole procedure, including the prior, but still assumed that the models chosen by the first author for the test were representative of real lensing galaxies. A similar test using current galaxy-formation simulations is desirable but technically formidable; however, we carry out a simple version of such a test below.

3. RESULTS

Our H_0^{-1} distribution is shown in Figure 1 and may be summarized as

$$H_0^{-1} = 13.5^{+2.5}_{-1.2}\ \mathrm{Gyr} \quad (H_0 = 72^{+8}_{-11}\ \mathrm{km\ s^{-1}\ Mpc^{-1}}) \quad (2)$$

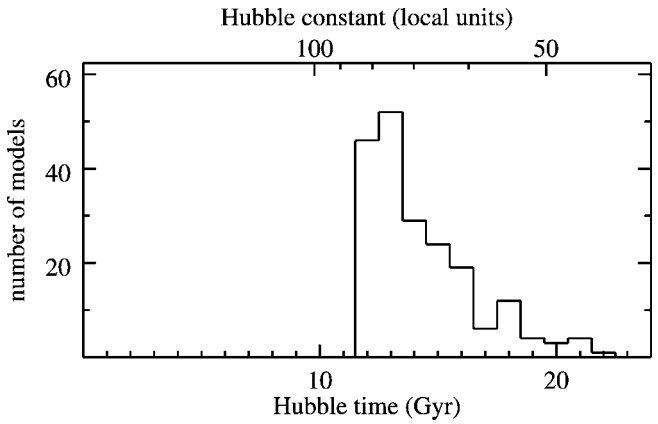

FIG. 1.—Histogram of the ensemble of H_0^{-1} values. The unbinned distribution gives $H_0^{-1} = 13.5^{+2.5}_{-1.2}$ Gyr at 68% confidence and $13.5^{+5.6}_{-1.6}$ Gyr at 90% confidence.

at 68% confidence and $13.5^{+5.6}_{-1.6}$ Gyr at 90% confidence. This estimate neglects measurement errors in the time delays. However, we have verified by repeating the analysis with perturbed time delays that the effect of measurement errors is very small. Astrometric errors are also very small.

Figure 1 is consistent with the analogous Figures 8 and 11 in Saha & Williams (2004), which derive from two time delay quads and four doubles considered separately. But the constraints do not improve as much as simple $1/\sqrt{N}$ would predict. In fact, the uncertainties are far from Gaussian, and some lensing configurations are much more useful than others. Saha et al. (2006) discuss this point in more detail and conclude that a 5% uncertainty on H_0^{-1} is possible using 11 lenses, provided the lenses all have favorable configurations.

Figure 2 shows ensemble average mass distributions for the 10 lenses. Notice that some lenses, especially B1115+080, B1104−181, and B1520+530, have twisting isodensity contours and/or radially dependent ellipticities, features that are not included in parameterized models.

The lens galaxies have varying amounts of dark matter. This follows from Ferreras et al. (2005), who compare the total-mass profiles of 18 lensing galaxies, including six from the present sample, with stellar-mass profiles from population-evolution models. (The work assumed $H_0^{-1} = 14$ Gyr, which is well within our uncertainties, and hence the results are valid for the models here.) From their Table 1, we see that out to $\sim 3R_{\mathrm{eff}}$, B1520+530 is mainly stars, B1115+080, B1608+656, and B2149−274 have significant nonstellar mass, while J0951+263 and B1104−181 are dominated by dark matter.

4. LENS MODELS COMPARED WITH A SIMULATION

We now address a simplified version of the question: are our lens models typical of current galaxy-formation simulations?

The details of gas dynamics, star formation, active galactic nucleus formation, and feedback on galaxy scales are still uncertain. With this caveat in mind, we consider a single high-resolution galaxy, extracted from an N-body cosmological simulation and then resimulated using the TreeSPH GASOLINE code (Wadsley et al. 2004) including gas cooling, star formation, supernova feedback, and UV background. The galaxy is an E1 or E2 triaxial elliptical dominated by stars in the inner region but overall ∼80% dark matter (Macciò et al. 2006). Orienting this galaxy randomly and ray-tracing with random sources (Macciò 2005), we generated about 500 quads and 10,000 doubles, and calculated time delays for each of these.

As equation (1) suggests, time delays generated from a single

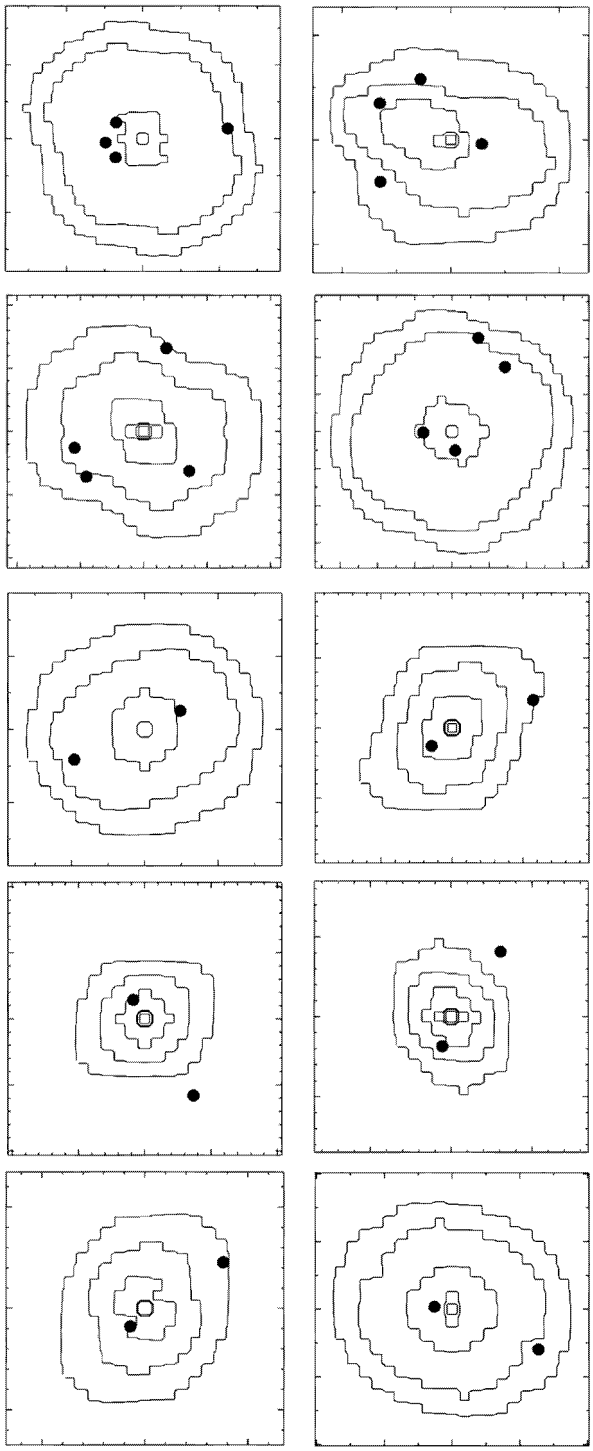

FIG. 2.—Ensemble-average mass maps of the lenses: J0911+055 (*upper left*), B1608+656 (*upper right*), B1115+080, B0957+561, B1104−181, B1520+530, B2149−274, B1600+434, J0951+263, and B0218+357. The larger tick marks in each panel correspond to 1″. The contours are in logarithmic steps, with critical density corresponding to the third contour from the outside.

galaxy will range over a factor of only a few and cannot be directly compared with the observed time delays, which range over a factor of 40. We therefore consider a dimensionless form of the time delay φ, given by

$$H_0 \Delta t = \varphi \frac{1}{16} (\theta_1 + \theta_2)^2 D, \quad (3)$$

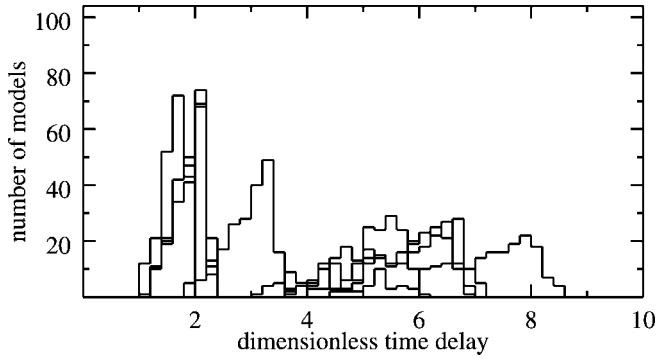

FIG. 3.—Histograms of φ for all 10 lenses. J0911+055, B1608+656, and B1115+080 all peak around 2. B0957+561 peaks around 3. B1104−181 peaks around 2. B1520+530, B1600+434, J0951+263, and B0218+357 all peak around 6. B2149−274 peaks around 8.

where θ_1, θ_2 are the lens-centric distances (in radians) of the first and last images to arrive, Δt is the observed time delay between them, and D is the usual distance factor in lensing. This factors out the dependence of the time delay on cosmology (through H_0 and D) and on the scale of the lens [through $(\theta_1 + \theta_2)^2$], leaving φ dependent only on the shape and steepness of the lens and on the source position with respect to the caustics (Saha 2004).

Figure 3 shows the histograms of φ in our lens-model ensembles. The quads all peak around 2, while the doubles mostly peak around 5–8; the exceptions are B0957+561 peaking around 3 and B1104−181 peaking around 2. Since B0957+561 is in a cluster, it is plausible that the mass profile is unusually shallow, thus reducing the time delay through the well-known steepness degeneracy. The low value for B1104−181 is more puzzling. Figure 4 is simpler, showing the probability distributions of φ for doubles and quads generated by the single simulated galaxy.

Figures 3 and 4 are not quite equivalent, but we can think of both as derived from an underlying prob(φ | galaxy, lensing obs). Each histogram in Figure 3 weights this probability distribution by observation selection effects and by the PixeLens prior, and then marginalizes over galaxies while holding the lensing observables fixed. Figure 4 marginalizes over lensing observables (separately for doubles and quads) while holding the galaxy fixed. Bearing this difference in mind, the simulated galaxy appears typical of our lens models. The most noticeable difference is the absence of observed quads with φ close to zero; but that is an expected observational selection effect, because very short time delays are unlikely to be measured.

We conclude that the PixeLens prior, as far as this preliminary experiment can reveal, is consistent with galaxy-formation sim-

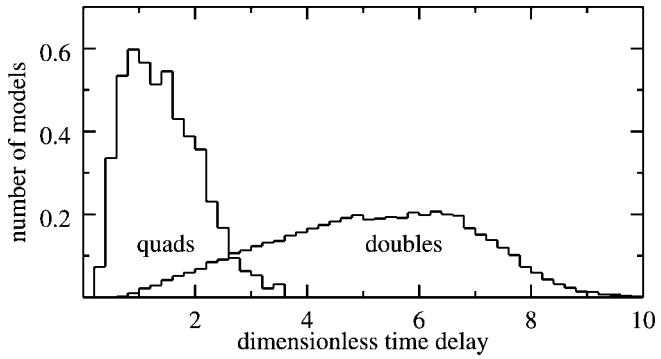

FIG. 4.—Probability distribution of φ for the simulated galaxy. Doubles and quads are normalized separately.

ulations. Further comparisons with simulated galaxies and fine-tuning of the prior are desirable in future work.

5. DISCUSSION

We have expressed our main result (Fig. 1) preferentially in terms of H_0^{-1} rather than H_0 because the former appears more naturally in lensing theory. But it is interesting to continue with H_0^{-1} in comparing with other techniques, because H_0^{-1} has a simple interpretation quite generally: it is $a/\dot{a}$ or the doubling time for metric distances at the current expansion rate. Coincidentally,[4] in the concordance cosmology ($K = 0$, $\Omega_m \simeq \frac{1}{4}$, $w = -1$) H_0^{-1} also equals the expansion age of the universe, within uncertainties. In particular, H_0^{-1} estimates can be immediately compared with globular cluster ages, such as in Krauss & Chaboyer (2003).

The well-known recent measurements of H_0^{-1}, expressed in gigayears, are:

1. 13.6 ± 1.5 from Freedman et al. (2001), who combine several different indicators calibrated using Cepheids;
2. 15.7 ± 0.3 (statistical) $\pm$ 1.2 (systematic) from Sandage et al. (2006), who use Type Ia supernova distances calibrated using Cepheids;
3. 13.6 ± 0.6 from Spergel et al. (2006), who use the cosmic microwave background (CMB) fluctuation spectrum.

[4] Although a spoof paper by Scott (2006) develops a conspiracy theory for this.

Our result is consistent with any of these.

It is worth noting, however, that the Hubble parameter appears in very different guises in different techniques. The distance-ladder methods measure the local cosmological expansion rate, independent of the global geometry. By contrast, in the CMB, H_0^{-1} is one parameter in a global cosmological model. Lensing is different again: here one assumes a global geometry and then measures a single scale parameter. The same is true of Sunyaev-Zel'dovich and X-ray clusters. The latter technique has made significant progress recently (Jones et al. 2005) but thus far still relies on strong assumptions: spherical symmetry of the cluster potential and hydrostatic equilibrium of the gas. In principle, lensing time delays can determine the global geometry as well (Refsdal 1966), but the amount of data needed is not observationally viable yet.

Whether lensing time delays can get the uncertainties in the Hubble parameter down to the 5% level is an open question. Maybe galaxy-lens models can be constrained enough to determine H_0^{-1} to better than 5%, thus making lensing the preferred method (Schechter 2004); or maybe the approach is best used in reverse, inputting H_0^{-1} to constrain galaxy structure (Kochanek et al. 2006). Fortunately, either outcome is worthwhile, and the basic technique will be the same. So whether the optimists or the pessimists are right, the usual cliches of "more data!" (time delay measurements) and "more theory!" (lens models) are both apt.

REFERENCES

Barkana, R. 1997, ApJ, 489, 21
Bernstein, G., & Fischer, P. 1999, AJ, 118, 14
Biggs, A. D., Browne, I. W. A., Helbig, P., Koopmans, L. V. E., Wilkinson, P. N., & Perley, R. A. 1999, MNRAS, 304, 349
Burud, I., et al. 2000, ApJ, 544, 117
———. 2002a, A&A, 383, 71
———. 2002b, A&A, 391, 481
Cohen, A. S., Hewitt, J. N., Moore, C. B., & Haarsma, D. B. 2000, ApJ, 545, 578
Courbin, F. 2006, in ASP Conf. Ser. 326, Gravitational Lensing: A Unique Tool for Cosmology, ed. D. Valls-Gabaud & J.-P. Kneib (San Francisco: ASP), in press (astro-ph/0304497)
Courbin, F., Meylan, G., Kneib, J.-P., & Lidman, C. 2002, ApJ, 575, 95
Fassnacht, C. D., Xanthopoulos, E., Koopmans, L. V. E., & Rusin, D. 2002, ApJ, 581, 823
Ferreras, I., Saha, P., & Williams, L. L. R. 2005, ApJ, 623, L5
Freedman, W. L., et al. 2001, ApJ, 553, 47
Hjorth, J., et al. 2002, ApJ, 572, L11
Jakobsson, P., Hjorth, J., Burud, I., Letawe, G., Lidman, C., & Courbin, F. 2005, A&A, 431, 103
Jones, M. E., et al. 2005, MNRAS, 357, 518
Keeton, C. R., Burles, S., Schechter, P. L., & Wambsganss, J. 2006, ApJ, 639, 1
Kochanek, C. S., Morgan, N. D., Falco, E. E., McLeod, B. A., Winn, J. N., Dembicky, J., & Ketzeback, B. 2006, ApJ, 640, 47
Koopmans, L. V. E., Treu, T., Bolton, A. S., Burles, S., & Moustakas, L. A. 2006, ApJ, in press (astro-ph/0601628)
Krauss, L. M., & Chaboyer, B. 2003, Science, 299, 65
Kundić, T., et al. 1997, ApJ, 482, 75
Lovell, J. E. J., Jauncey, D. L., Reynolds, J. E., Wieringa, M. H., King, E. A., Tzioumis, A. K., McCulloch, P. M., & Edwards, P. G. 1998, ApJ, 508, L51
Macciò, A. V. 2005, MNRAS, 361, 1250
Macciò, A. V., Moore, B., Stadel, J., & Diemand, J. 2006, MNRAS, 366, 1529
Morgan, N. D., Kochanek, C. S., Falco, E. E., & Dai, X. 2006, ApJ, submitted (astro-ph/0605321)
Ofek, E. O., & Maoz, D. 2003, ApJ, 594, 101
Oguri, M., et al. 2004, ApJ, 605, 78
Oscoz, A., et al. 2001, ApJ, 552, 81
Raychaudhury, S., Saha, P., & Williams, L. L. R. 2003, AJ, 126, 29
Refsdal, S. 1964, MNRAS, 128, 307
———. 1966, MNRAS, 132, 101
Saha, P. 2004, A&A, 414, 425
Saha, P., Courbin, F., Sluse, D., Dye, S., & Meylan, G. 2006, A&A, 450, 461
Saha, P., & Williams, L. L. R. 2003, AJ, 125, 2769
———. 2004, AJ, 127, 2604
Sandage, A., Tammann, G. A., Saha, A., Reindl, B., Macchetto, F. D., & Panagia, N. 2006, ApJ, submitted (astro-ph/0603647)
Scott, D. 2006, preprint (astro-ph/0604011)
Schechter, P. L. 2004, in IAU Symp. 225, The Impact of Gravitational Lensing on Cosmology, ed. Y. Mellier & G. Meylan (Cambridge: Cambridge Univ. Press), 281
Schechter, P. L., et al. 1997, ApJ, 475, L85
Spergel, D. N., et al. 2006, ApJ, submitted (astro-ph/0603449)
Ullán, A., Goicoechea, L. J., Zheleznyak, A. P., Koptelova, E., Bruevich, V. V., Akhunov, T., & Burkhonov, O. 2006, A&A, 452, 25
Vuissoz, C., et al. 2006, A&A, submitted (astro-ph/0606317)
Wadsley, J. W., Stadel, J., & Quinn, T. 2004, NewA, 9, 137
Williams, L. L. R., & Saha, P. 2000, AJ, 119, 439
Winn, J. N., Kochanek, C. S., McLeod, B. A., Falco, E. E., Impey, C. D., & Rix, H.-W. 2002, ApJ, 575, 103